MACHINE LEARNING PREDICTION OF SOIL PARTICLE SIZE DISTRIBUTION FROM SMARTPHONE IMAGES

Enrico Soranzo
Department of Landscape, Water and Infrastructure, BOKU University, Austria. E-mail: enrico.soranzo@boku.ac.at

Keywords: Convolutional neural network, soil particle size distribution, transfer learning, image analysis.

1 Introduction

In geotechnical engineering, soil classification is primarily based on the particle size distribution (PSD) curve for coarse soils and plasticity for fine soils (ISO 14688-1, 2017; ISO14688-2, 2017; ISO17892-4, 2016 and ISO17892-12, 2018). Traditional methods, such as sieving and sedimentation, are effective but labor-intensive. PSD is crucial because it affects soil properties like residual water content, hydraulic conductivity and groutability (Hwang, 2006; Vipulanandan, 2009).

Recent advancements have introduced alternative methods, including gamma-ray attenuation, reflectance of visible and infrared radiation, and image analysis, to estimate PSD (Zuo, 2000). However, these methods face limitations related to accuracy, applicability and costs. Traditional image processing techniques have been used to classify soil textures, but they often struggle with lower accuracy and the inability to predict the full PSD curve.

Convolutional neural networks (CNNs) have shown promise in image analysis tasks. Studies have used CNNs to classify soil images into various texture classes. For example, Buscombe, 2020 developed a machine-learning framework to estimate sedimentological properties from photographic imagery, while Lang, 2021 introduced a CNN for grain size analysis of river systems using aerial images. Despite these advancements, most CNN-based methods focus on soil texture classification rather than predicting PSD.

Soranzo et al., 2025 focused on both coarse and fine soils, deriving the ground truth from standardized geotechnical testing and describing the PSD through curve fitting parameters. By employing MobileNet pre-trained on ImageNet with additional layers for transfer learning and capturing soil images under standardized lab conditions, the study provided a robust and efficient method for PSD prediction.

However, when the model was tested with completely new, unseen data from different geographical settings, its performance slightly lagged. To address this, the study incorporates some of the new data into the training process. Additionally, further improvements are made through data augmentation by adjusting saturation and hue levels. The model also employs 5-fold cross-validation. By incorporating these technical advancements, the practical contribution of the model and its potential for larger-scale industrial deployment through the web application is enhanced.

2 Materials and Methods

In this study, soil samples primarily collected near Vienna, Austria and Frankfurt, Germany were analyzed to determine their particle size distributions (PSDs). Close-range photos of the soil samples and their PSDs were used as the inputs and outputs for the model.

2.1 Data Acquisition

2.1.1 Input Data

Images were taken with smartphone cameras in a dark chamber (Figure 1). The smartphones were placed on top of the chamber, and photos were taken from a 45×45 mm opening at a distance of 210 mm from the soil surface, based on Azadnia, 2022. Different smartphone cameras have varying angles-of-view, so different soil areas were photographed from the same distance. The inner ground dimensions were chosen to accommodate the areas photographed by the smartphones.

The soil samples were homogenized using a cement mixer and oven-dried. The soil was dry-pluviated. Images were taken with Motorola Edge, Samsung A52 and iPhone 14 smartphones with resolutions of 4000×1800, 6936×9248 and 4032×3024 pixels, respectively. Multiple pictures of the same soil were taken to avoid biases, with the soil surface altered between pictures using various tools. A total of 170 pictures were taken and imported as three-dimensional tensors, where the third dimension corresponds to the three color channels.

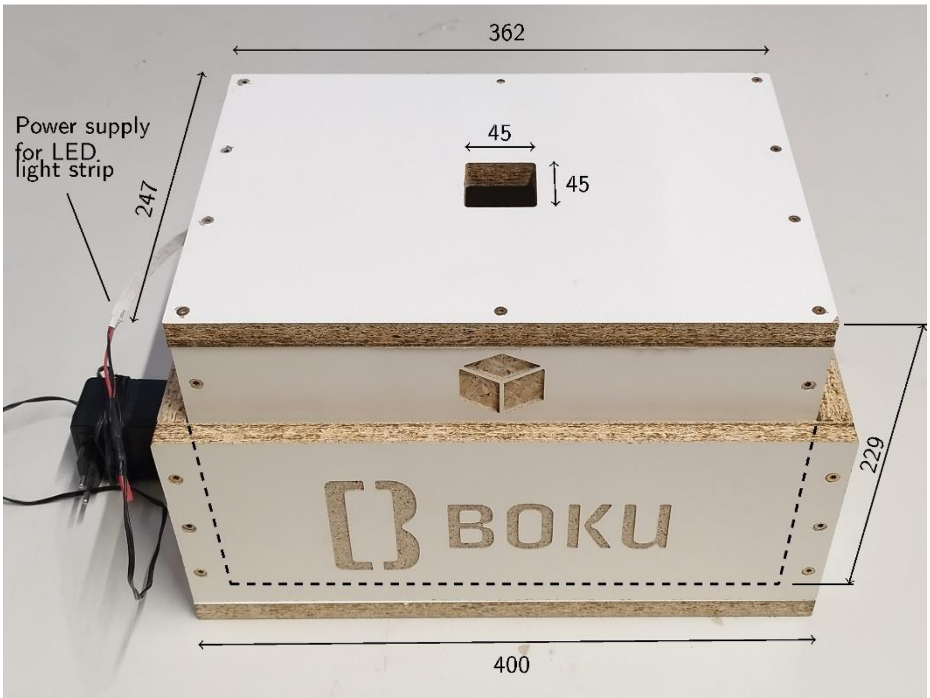

Figure 1. Experimental setup for capturing soil images. The smartphone is positioned on top of a dark chamber to minimize light reflection, with photos taken through a 45×45 mm opening. The distance from the soil surface to the camera lens is set to about 210 mm (Soranzo et al., 2025)

2.1.2 Scaling

To standardize data, it is essential to calibrate the pixel density of each smartphone by photographing a ruler or scale from the opening and measuring the pixels per mm (PPM), as shown in Figure 2. The smartphone images were resized to a common pixel density of 4.6 PPM. The images were then cropped into 400×400 pixel squares to simplify convolutional and pooling operations.

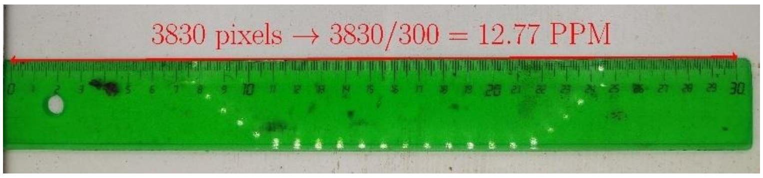

Figure 2. Example calibration of the pixel density. A ruler is inserted into the dark chamber. The number of pixels for a given length are measured and the pixel density is calculated

2.1.3 Output Data

The soil samples consisted of 56 silty, sandy, and gravelly soils. The average clay, silt, sand and gravel contents were 2.7%, 22.4%, 41.6% and 31.6%, respectively. PSD curves were obtained by sieving for coarse fractions and by the hydrometer sedimentation method for fine fractions. The coefficients of uniformity and curvature of the curves varied between $C_U \in [1.9, 248.5]$ and $C_C \in [0.1, 49.4]$. The PSDs were fitted with the Weibull distribution, requiring only two parameters:

$$F(d \leq d_i) = 1 - \exp\left[-\left(\frac{d_i}{b}\right)^c\right] \quad (1)$$

where d is the particle diameter finer than d_i, b and c are fitting parameters. The parameters are comprised in the ranges $b \in [0.01, 39.561]$ and $c \in [0.392, 3.284]$. The natural logarithm of b is used as the output variable to stabilize the variance.

2.2 Convolutional Neural Network: MobileNet

MobileNet (Howard et al., 2017), a lightweight and efficient CNN, was utilized for this study. It was implemented using TensorFlow in Python 3.9 (Van Rossum et al., 2009) and trained with GPU acceleration on a NVIDIA GeForce RTX 3060 graphic card. MobileNet's depth-wise separable convolution divides the convolution process into depth-wise and point-wise convolutions, making it more efficient than traditional CNNs.

The MobileNet model was pre-trained on the ImageNet dataset (Deng, 2009), and transfer learning was employed to leverage knowledge from one task to improve performance on a related task. The pre-trained layers were frozen, and custom regression layers were added on top. The output of the base model was passed through a global average pooling layer, and a single CNN with double regression outputs was used to predict $ln(b)$ and c.

2.3 Data Splitting and Augmentation

90% of the images were used to train the CNN, and 10% were assigned to testing. The synthetic data augmentation techniques depicted in Figure 3 were applied to increase the training dataset size.

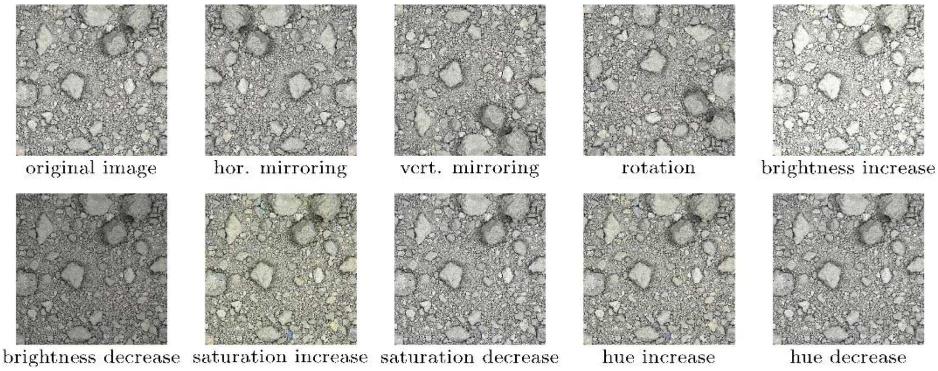

Figure 3. Visualization of the data augmentation techniques applied to the original image. Each transformation doubles the size of the dataset. Hence, 2^{10} = 512 pictures are created out of one original image

2.4 CNN Training

The CNNs featured 6,541,505 parameters of which 3,312,641 are trainable. To optimize the trainable parameters, the mean squared error (MSE) was minimized using the Adam optimizer with an initial learning rate of 0.001. Early stopping and model checkpointing were implemented to prevent overfitting, ensuring that the model generalizes well to unseen data. A mini-batch size of 32 was chosen. 5-fold cross-validation was conducted to ensure robustness and reliability of the model across different subsets of the data.

Once training was completed, the coefficient of determination (R^2) and mean absolute percentage error (MAPE) were computed for the training and test sets.

3 Results

Model training took approximately one day. The R^2 and MAPE values for $ln(b)$ and c were evaluated on both the training and testing datasets, by comparing the model's predictions for $ln(b)$ and c to the observations (Figure 4). The model's predictions align well with the expected values, with the dashed region representing a ±30% tolerance around the perfect prediction line. Specifically, the model achieved R^2 and MAPE of 1.000 and

2.3%, 0.885 and 12.9% on the training and test sets for $ln(b)$; R^2 and MAPE of 0.995 and 3.5%, 0.954 and 6.1% on the test set s for c.

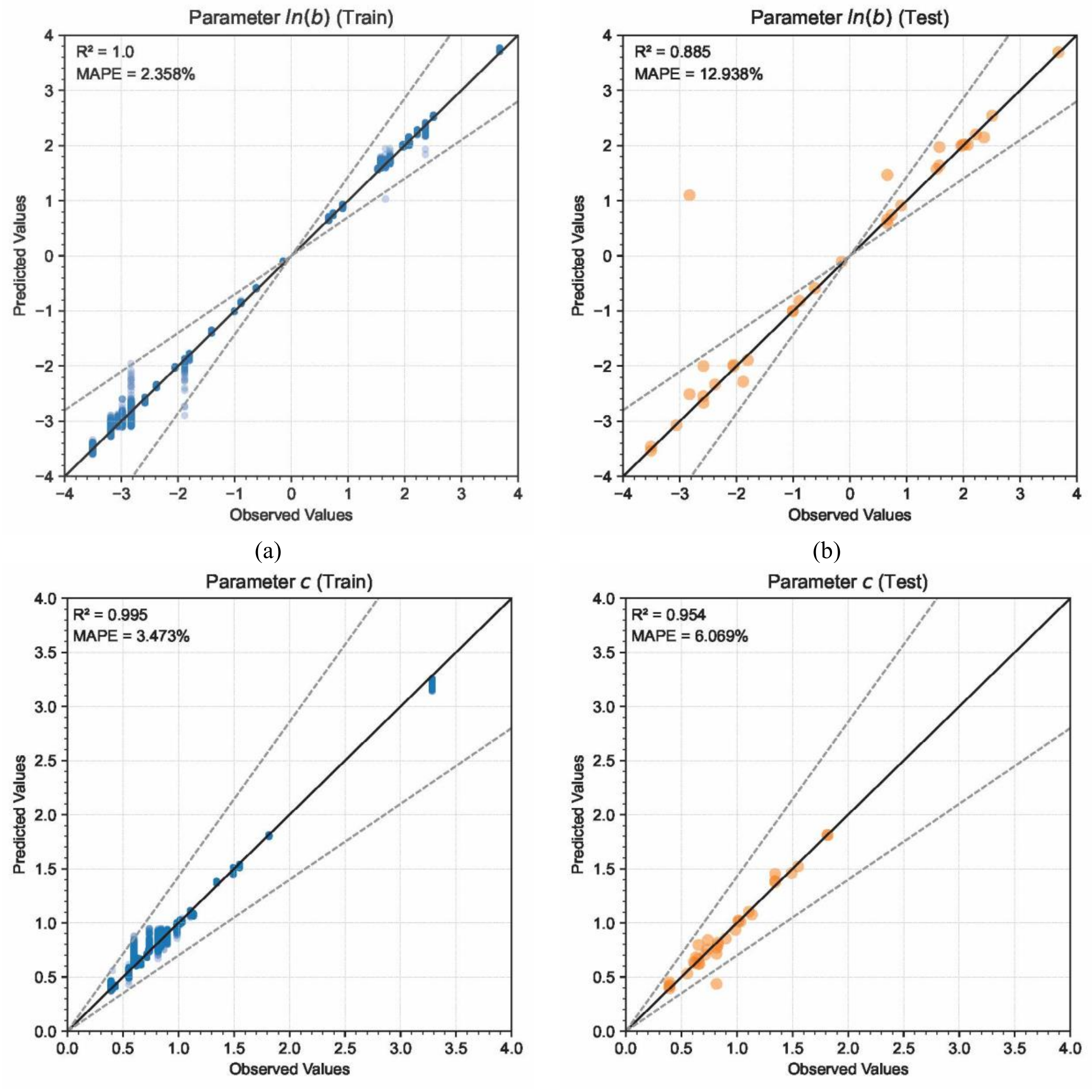

Figure 4. Model prediction of parameters $ln(b)$ and c in training (a, c) and test (b, d) against observed values

4 Web-App

A web application has been developed using Streamlit to deploy the model (https://soranz84-grai2.hf.space). The application allows users to upload soil images. It currently supports the three smartphones and resolutions listed in Section 2.1.1 as well as iPhone16 with resolution 4284×5712 (not yet used for model training). Once an image is uploaded, it is resized to the 4.6 PPM pixel density, then cropped to 400×400 pixels to match the CNN requirements. The processed image is fed into the model to predict $ln(b)$ and c which are then used to plot the PSD (Figure 5).

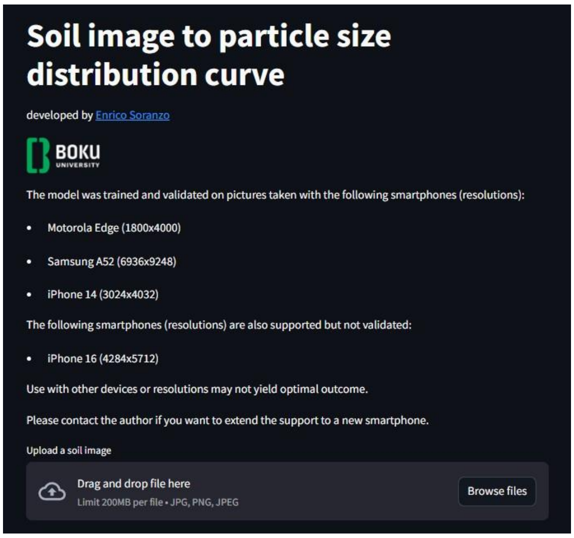

(a)

(b)

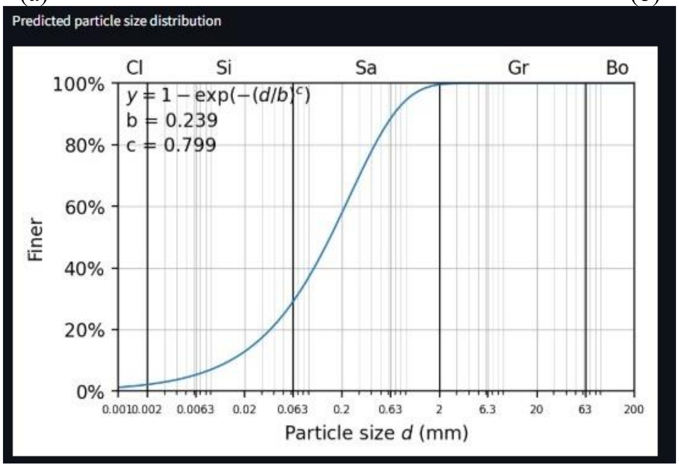

(c)

Figure 5. Screenshot from the developed web-app. The soil image is uploaded (a), scaled and cropped (b), and the PSD is shown, based on the predicted parameters (c)

5 Discussion and conclusions

This study presents a CNN for predicting the soil PSD based on smartphone images taken in a dark chamber. The main advantage of our tool is its ability to provide rapid and efficient predictions. The model is deployed online, allowing users to upload soil images and receive PSD predictions in real-time. This online deployment significantly contributes to realizing accessible and cost-effective soil analysis, aligning with our aim to provide high-quality results using readily available tools. Despite the limitation imposed by the pixel density value of 4.6 pixel per mm, our primary aim is to predict two curve parameters to interpolate the entire particle size distribution. Hence, even the content of finer particle sizes can be captured, provided that this is not too high.

The predictability of the fitting parameters implies our capability to generate values that closely align with the PSD interpolation. The model was tested on a wide spectrum of soils, demonstrating reliability and relevance. However, future research should include purely clayey soils (to improve the accuracy of the fines) and more samples from diverse geographic locations (to train the model on different particle textures).

The main conclusions are:

- The model provides rapid and efficient predictions of the PSD from soil images
- The model accurately interpolates the entire PSD curve
- The model was tested on a wide spectrum of soils
- The study demonstrates that high-quality soil analysis can be achieved with accessible and cost-effective tools
- Future studies should focus on including a broader range of smartphones with different camera specifications.

5.1 Acknowledgements

Funded by the European Union under the MSCA Staff Exchanges project 101182689 Geotechnical Resilience through Intelligent Design GRID. Views and opinions expressed are however those of the author(s) only and do not necessarily reflect those of the European Union or European Research Executive Agency (REA). Neither the European Union nor the granting authority can be held responsible for them. The author would like to thank Anand D'Souza of BOKU, Stefan Resch and Dennis Tegen of HPC for providing image data and particle size distributions to train the models.

5.2 References

Azadnia, R., Jahanbakhshi, A., Rashidi, S., Khajehzadeh, M., Bazyar, P. (2022) Developing an automated monitoring system for fast and accurate prediction of soil texture using an image-based deep learning network and machine vision system. *Measurement* 190, 110669. https://doi.org/10.1016/j.measurement.2021.110669},

Buscombe D. (2020) SediNet: a configurable deep learning model for mixed qualitative and quantitative optical granulometry. *Earth Surface Processes and Landforms* 45(3), 638–651. https://doi.org/10.1002/esp.4760

Deng, J., Dong, W., Socher, R., Li, L.-J., Li, K., Fei-Fei, L. (2009) *ImageNet: A Large-Scale Hierarchical Image Database*. CVPR09

Howard, A.G., Zhu, M., Chen, B., Kalenichenko, D., Wang, W., Weyand, T., Andreetto, M., Adam, H. (2017) MobileNets: Efficient Convolutional Neural Networks for Mobile Vision Applications. *CoRR* abs/1704.04861. https://doi.org/10.48550/arXiv.1704.04861

Hwang, S.I., Sang, P.H. (2006) Estimating relative hydraulic conductivity from lognormally distributed particle-size data. *Geoderma* 133(3), 421–430. https://doi.org/10.1016/j.geoderma.2005.08.006

ISO 14688-1 (2017) *Geotechnical investigation and testing — Identification and classification of soil — Part 1: Identification and description*. International Organization for Standardization

ISO14688-2 (2017) *Geotechnical investigation and testing — Identification and classification of soil — Part 2: Principles for a classification*. International Organization for Standardization

ISO17892-4 (2016) *Geotechnical investigation and testing — Laboratory testing of soil — Part 4: Determination of particle size distribution*. International Organization for Standardization

ISO17892-12 (2018) Geotechnical investigation and testing — Laboratory testing of soil — Part 12: Determination of liquid and plastic limits. International Organization for Standardization

Lang, N., Irniger, A., Rozniak, A., Hunziker, R., Wegner, J. D., Schindler, K. (2021) GRAINet: mapping grain size distributions in river beds from UAV images with convolutional neural networks. *Hydrology and Earth System Sciences* 25(5), 2567–2597. https://doi.org/10.5194/hess-25-2567-2021

Misra, D. (2020) Mish: A Self Regularized Non-Monotonic Activation Function. *arXiv*. https://arxiv.org/abs/1908.08681

Soranzo, E., Guardiani, C., Wu, W. (2025) Convolutional neural network prediction of the particle size distribution of soil from close-range images. *Soils and Foundations* 65(1), 101575. https://doi.org/10.1016/j.sandf.2025.101575

Van Rossum, G., Fred L.D. (2009) *Python 3 Reference Manual*. CreateSpace

Vipulanandan, C., Ozgurel, H.G. (2009) Simplified Relationships for Particle-Size Distribution and Permeation Groutability Limits for Soils. *Journal of Geotechnical and Geoenvironmental Engineering* 135(9), 1190–1197. https://doi.org/10.1061/(ASCE)GT.1943-5606.0000064

Zuo, Y., Erbach, D.C., Marley, S.J (2000) Soil structure evaluation by using a fiber-optic sensor. *Transactions of the American Society of Agricultural Engineers* 43(6), 1317–1322